ARTICLES

Journal of Semiconductors
(2020) 41, 122701
doi: 10.1088/1674-4926/41/12/122701

JOS

Effects of high temperature annealing and laser irradiation on activation rate of phosphorus

Shaojie Li[1, 2] and Peide Han[1, 2, †]

[1]Institute of Semiconductors, Chinese Academy of Sciences, Beijing 100083, China

[2]University of Chinese Academy of Sciences, Beijing 100049, China

Abstract: Thermal annealing and laser irradiation were used to study the activation rate of phosphorus in silicon after ion implantation. The activation rate refers to the ratio of activated impurity number to the total impurity number in the sample. After injecting phosphorus with the dose and energy (energy = 55 keV, dose = 3×10^{15} cm^{-2}), the samples were annealed at different temperatures, and laser irradiation experiments were performed after annealing. The experimental results showed that the activation rate of phosphorus was the highest at 850 °C, and the highest activation rate was 67%. Upon femtosecond laser irradiation samples after thermal annealing, while keeping the crystalline silicon surface without damage, the activation rate was improved. When the energy-flux density of the femtosecond laser was 0.65 kJ/cm^2, the activation rate was the highest, increasing from 67% to 74.81%.

Key words: thermal annealing; ion implantation; femtosecond laser; activation rate

Citation: S J Li and P D Han, Effects of high temperature annealing and laser irradiation on activation rate of phosphorus[J]. *J. Semicond.*, 2020, 41(12), 122701. http://doi.org/10.1088/1674-4926/41/12/122701

1. Introduction

As is known, after annealing at a certain temperature for a certain time, the implanted impurities may undergo a large extent of redistribution in the solid, and the normal solid-state diffusion is negligible at this time. This effect has been observed in several substances implanted into silicon, such as boron[1] and phosphorus[2] annealing in silicon. It indicates that this phenomenon results from an abnormal diffusion process, which includes a complex combination of material and dopant parameters, such as defect generation, dopant concentration, enhanced defect diffusion coefficient, migration and lattice rearrangement[3]. Many studies have been conducted on the activation of impurities during annealing[4–9]. After annealing at a lower temperature (400–500 °C), the sheet resistance begins to decrease, which can be attributed to the electrical activation of impurity atoms; while in the range of 500–600 °C, which increases with temperature. This phenomenon is known as reverse annealing[9]. It occurs as a result of the formation of complex defects, which requires an annealing temperature of 700 °C to be removed. In order to achieve the activation of the implanted impurities, the samples must be annealed at a temperature higher than 700 °C. However, there is little research focusing on annealing in high temperature processes. In the production of crystalline silicon solar energy, most of them are annealed at high-temperature conditions. Therefore, the high annealing temperature is more important for the production of crystalline silicon solar cells. In the production of high-efficiency crystalline silicon solar cells by implanting phosphorus ions into silicon, the annealing temperature is generally between 800–900 °C, and the time is generally around 30 min. However, no specific temperature parameters are specified. The phosphorus was implanted into P-type silicon, and the thermal annealing experiments were carried out under different high temperature conditions. The experimental condition with the highest activation rate of phosphorus ions can be obtained through experiments. When the annealing was performed at 850 °C, the activation rate of 67% for phosphorus was the highest.

How do you further improve the activation rate of phosphorus under the optimal annealing temperature? This has important guiding significance for further improving the efficiency of crystalline silicon solar cells and applying it to industrial production. Femtosecond (fs) laser irradiation is one of the most attractive manufacturing methods to produce black silicon (B-Si)[10–12]. However, since the impurity separation coefficient of sulfur atoms in the silicon substrate is extremely small (~ 10^{-5}), the solid solubility is extremely low (3×10^{16} cm^{-3})[13]. It is difficult to construct a p–n junction based on a semiconductor device, which is not conducive to the improvement of crystalline solar cell efficiency. Compared with sulfur, phosphorous shows the following advantages in the silicon substrate. Firstly, phosphorous has a larger separation coefficient (0.36) and a higher annealing solid solubility (1.3×10^{21} cm^{-3})[14]. Secondly, since the atomic radius of phosphorus is close to that of silicon, the lattice distortion of the silicon substrate caused by phosphorus doping is much smaller. Since femtosecond laser irradiation can increase the activation amount of sulfur impurities, it is speculated that femtosecond laser irradiation should increase the activation amount of phosphorus impurities, thereby increasing the activation rate of phosphorus. This provides a method for improving the efficiency of high-efficiency crystalline silicon solar cells in the future. The femtosecond laser was used to irradiate the thermally annealed samples, revealing that

Correspondence to: P D Han, pdhan@red.semi.ac.cn
Received 22 APRIL 2020; Revised 11 AUGUST 2020.
©2020 Chinese Institute of Electronics

the activation rate of phosphorus after laser irradiation was improved compared with that before the experiment. While ensuring that the phosphorus-doped layer does not cause significant damage, the activation rate of phosphorus was increased from 67% to 74.81%, and the activation rate was increased by 7.83%. It illustrated that the femtosecond laser can indeed increase the activation rate of phosphorus.

2. Experimental section

2.1. Thermal annealing

In the experiment, P-type <100> silicon wafers with a resistivity of 1–10 Ω•cm were used. During the ion implantation, the samples oriented with their normal tilted 7° relative to the incident beam in order to avoid channeling effects. The silicon wafers were implanted with phosphorous at room temperature (energy = 55 keV, dose = 3×10^{15} cm^{-2}). Then these samples were isothermally annealed at various temperatures (800–950 °C) for 30 min in a nitrogen atmosphere.

After annealing, the electrochemical capacitance–voltage profiler (ECV) was used to measure the activated concentration, and the secondary ion mass spectroscopy (SIMS) was applied to measure the total concentration. Rutherford backscattering spectrometry (RBS) was used to measure the channel energy spectrum at different annealing temperatures.

2.2. Femtosecond laser irradiation

The samples were annealed at the temperature with the highest activation rate. Then they were irradiated by a femtosecond laser in vacuum. In order to obtain large-area samples, the vacuum cavity was mounted on a two-dimensional translation stage controlled by a computer program. The silicon wafers were moved in the S-line sweep at a rate of 1 mm/s.

Raman spectra was used to measure the crystallinity of the surface irradiated by the femtosecond laser. The ECV was applied to measure the activated concentration and the SIMS was used to measure the total concentration.

The ECV instrument used CVP21 produced by the French Wep Company, and NH_4F/HF solution was used as the electrolyte. The instrument of SIMS was equipped with a CAMECA IMS-4F device using a 5-keV Cs beam. The experimental equipment for Rutherford backscatter analysis consists of a small particle accelerator, a vacuum target chamber, a particle detector, and electronic circuits. The accelerator provides He ions with 2 MeV energy and 4 to 5 nA, and the vacuum of the target chamber is 10^{-5} Pa. In this work, a Horiba Jobin–Yvon Raman system with a 488 nm laser was used to characterize all samples. Raman spectra were taken at room temperature with a monochromator equipped with a 600 lines/mm grating and excited power 2 mW. The light source used in the experiment of the femtosecond laser was a Ti:sapphire femtosecond laser amplifier (800 nm center wavelength, 120 fs pulse duration, and 1 kHz repetition rate).

The experimental steps are shown in Fig. 1.

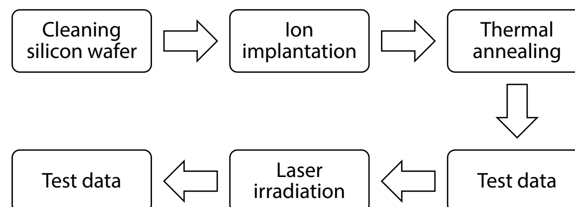

Fig. 1. The experimental steps.

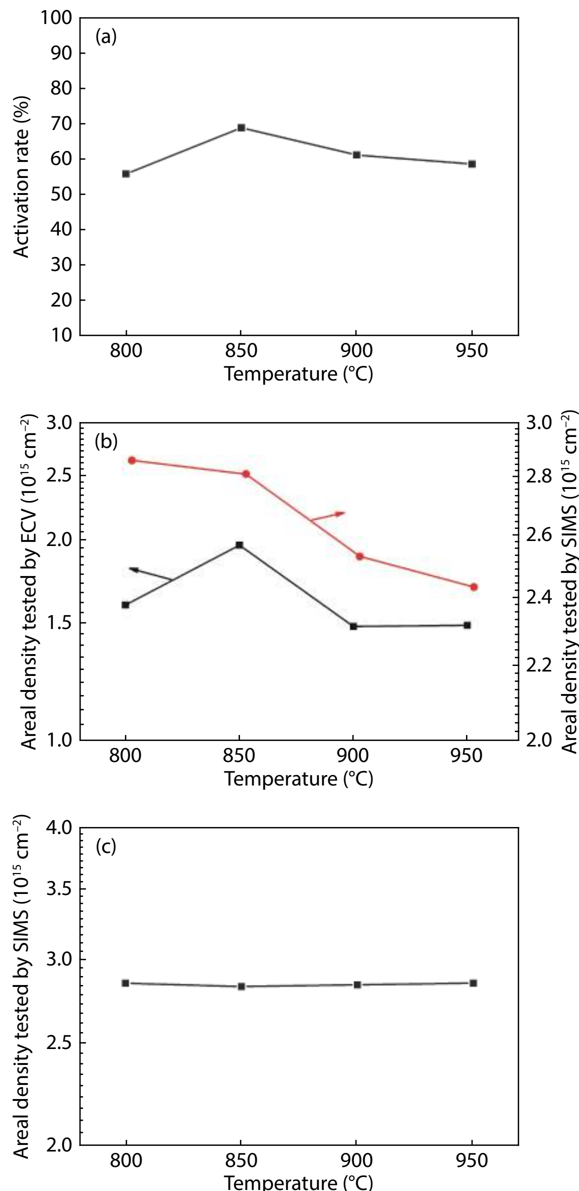

Fig. 2. (a) The activation rate of phosphorus at different temperatures. (b) Areal density of phosphorus of ECV and SIMS before the junction depth at different temperatures. (c) Areal density of phosphorus of SIMS at different temperatures.

3. Results and discussion

Fig. 2(a) shows an image for the activation rate of phosphorus at different temperatures. The activation rate of phosphorus reached the highest under the condition of 850 °C. Fig. 2(b) exhibits that the areal density of phosphorus tested by ECV was the highest 850 °C, that is, the activated concentration of phosphorus measured at this temperature was the highest, which can explain the highest activation rate at 850 °C. Fig. 2(b) also shows that the areal density of phosphorus impurities before the junction depth of SIMS test was decreased with increasing temperature. The reason for this phenomenon is that as the temperature increases, more and more phosphorus impurities diffuse behind the junction depth. But the total phosphorus impurity concentration does

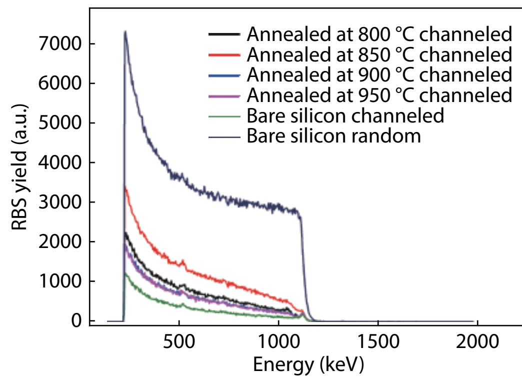

Fig. 3. (Color online) RBS images at different temperatures.

not change. Fig. 2(c) shows the areal density of phosphorus impurities of the SIMS test, and it can fully illustrate this phenomenon.

The diffusion of high concentration phosphorus in silicon during annealing after implantation is a complex phenomenon. First, it is not only the substitution-interstitial (S-I) mechanism but also the vacancy mechanism that must be considered because of the high-concentration of phosphorus[15]. Second, phosphorus exhibits transfer enhanced diffusion (TED), which is due to {311} self-interstitial clusters induced by ion implantation damage[16]. TED is a process due to the interaction between dopants and interstitials that are released during the occurrence of the Ostwald ripening process of defects[16]. Third, following amorphization induced by high-dose implantation, end-of-range (EOR) dislocations (Type II defects) are formed at the amorphous/crystalline (a/c) interface[17]. EOR dislocations act as both a sink for and source of self-interstitials, and hence affect TED[18]. In addition, phosphorus clusters should be considered[19]. Similar to boron clusters[20], under self-interstitial oversaturation caused by ion implantation, phosphorus clusters can occur even if the concentration is far below the solid solubility limit. Then, during the diffusion process, the phosphorus clusters are dissolved to produce self-interstitials, which also contributes to TED[19]. These phenomena make it difficult for the simulation of high-concentration phosphorus diffusion. A basic P-diffusion model[21] was adopted, including a vacancy mechanism, the TED model with Oswald ripening, and the model for EOR dislocations that affect TED. The accumulation of phosphorus clusters was also taken into account in the basic P-diffusion mode. The phosphorus diffusion model is the same as the method described in Ref. [21]. Literature theory[21] can basically explain the process of phosphorus diffusion.

Fig. 3 shows the RBS images of ion implanted silicon wafers at different temperatures. It was observed that the interstitial impurities were the most at 850 °C. The experimental conditions for the number of interstitial impurities in the sample were as follows: 850 °C > 800 °C > 900 °C > 950 °C. If the interstitial impurities are mainly phosphorous interstitial impurities, RBS indicates that the activated concentration of phosphorus was the lowest at 850 °C, which is inconsistent with the measured data of ECV. If the interstitial impurities are mainly silicon interstitial impurities, it indicates that under the condition of 850 °C, the activated concentration of phosphorus was the highest, because the silicon in the interstitial impurities is mainly caused by the substitution of the phosphorus impurities. It is consistent with the maximum number of activated phosphorus impurities under the condition of 850 °C in the ECV measure. Therefore, interstitial impurities are mainly silicon interstitial impurities[9].

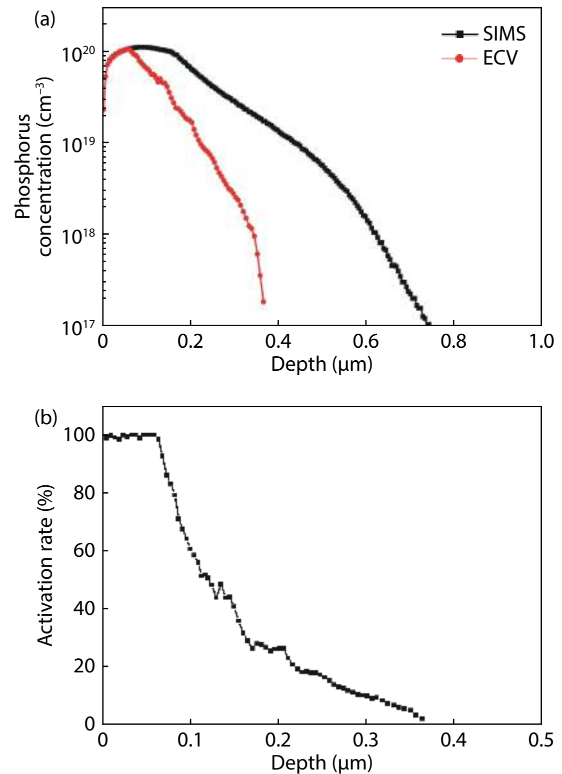

Fig. 4. (Color online) (a) ECV and SIMS measured results at 850 °C. (b) The activation rate with thickness at 850 °C.

The energy and yield of different elements are different after backscattering, which is reflected in different positions on the RBS[22] (abscissa is energy, ordinate is counting yield), that is, different elements appear at different energy positions, heavy elements appear at high-energy positions, and light elements appear at low-energy positions. In general, the energy spectrum scattered by impurity elements in the measured sample shows a Gaussian distribution peak in the RBS energy spectrum, which is obviously different from that of the substrate element. The incident ion beam used He ion beam. The difference between the atomic numbers of phosphorus and silicon is 1, and the atomic number of He is 2. When the He ion beam was used to strike the samples, the spectral line of the element silicon will interfere with that of the element phosphorus, that is, the He ion beam cannot distinguish between the silicon impurities and the phosphorus impurities in the interstitial impurities. In Fig. 3, the energy spectrum lines of silicon and phosphorus were superimposed together; that is, there was no Gaussian distribution peak. Therefore, it is impossible to calculate the concentration of phosphorus interstitial impurities and silicon interstitial impurities. The RBS energy spectrum revealed that at 850 °C, the interstitial impurities were the most, and the interstitial impurities were mainly silicon[9]. Therefore, at 850 °C, the activated concentration of phosphorus was the highest and the activation rate of phosphorus was the highest.

Fig. 4(a) shows the measured results of ECV and SIMS at 850 °C. The activated concentration of phosphorus at the surface was the highest. As the depth was increased, the activated concentration was decreased. Fig. 4(b) shows the

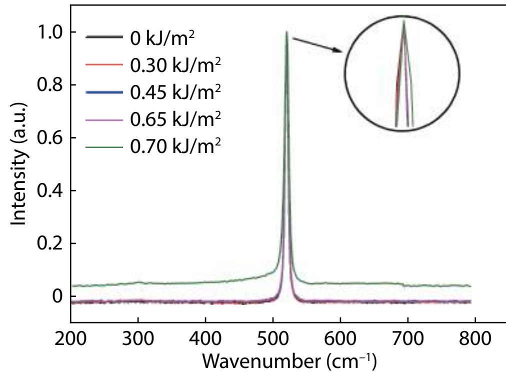

Fig. 5. (Color online) Raman spectra of samples under different energy-flux densities.

change of activation rate with depth at 850 °C. From Fig. 4(b), it can be seen that the activation rate showed a downward trend with the increase of the depth. It is verified that the diffusion after a certain depth in the process of thermal annealing is dominated by interstitial diffusion[15].

Why doesn't the activated phosphorus in the high-concentration area diffuse? A qualitative explanation is as follows[8].

In the process of deactivation in the high concentration area, it is assumed that the mobile $(P\text{-}V)^-$ reacts with the replacement phosphorus (P_s^+) to form a P_2V cluster and kick out I (I refers to interstitial silicon), i.e.

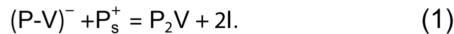

$$(P\text{-}V)^- + P_s^+ = P_2V + 2I. \quad (1)$$

This reaction generates two I; and one I can be used to form a $(P\text{-}V)^-$, the other interstitial silicon will remain. Therefore, this cycle generates one additional I. However, the resulting I will actually diffuse out of this area. If one of the two I, which are generated in the reaction, goes outside without reacting or vanishes at the surface, additional I cannot be expected in the high-concentration region. It is plausible that the rationality of I disappearing in a high concentration region or on the surface is more than 50%. Furthermore, if $(P\text{-}V)^-$ diffusion is outside the high-concentration area, it means that there is no enough I generation source, and there is no way to generate enough $(P\text{-}V)^-$. This may explain that why the activated phosphorus does not diffuse in the high concentration area.

The femtosecond laser has ultra-high energy, and its interaction with matter is an instant process. The process of the femtosecond laser and the silicon surface is as follows: (1) the pulse energy is quickly deposited on the silicon surface within the femtosecond time scale; (2) the electrons absorb ultra-high pulse energy and rapidly warm up and ionize into electron gas; (3) the high energy electron gas transfers energy to surrounding "cold" atoms through electron–photon coupling in the order of picoseconds to achieve energy transfer[23].

Fig. 5 is the normalized Raman image under different energy-flux densities. The sample under the energy-flux density of 0.7 kJ/m^2 had obvious background noise, but the Raman peak was only 520 cm^{-1}, which means that under this energy-flux density, only the characteristic peak of crystalline silicon, but no amorphous peak was formed. This also showed that the surface has energy damage, which is, however, not enough to produce lattice distortion. In addition, except for the energy-flux density of 0.7 kJ/m^2, the Raman spectra of

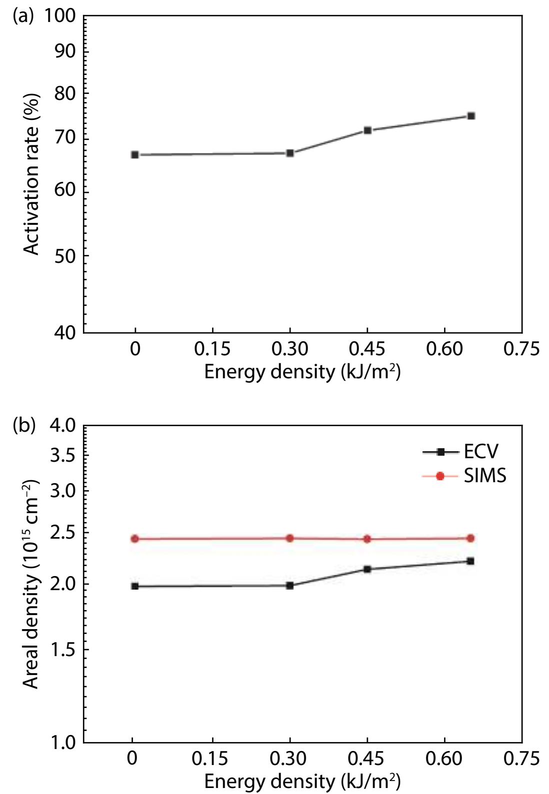

Fig. 6. (a) The activation rate of phosphorus at different energy-flux densities. (b) Areal density of phosphorus of ECV and SIMS at different energy-flux densities.

the remaining energy-flux densities were almost the same, indicating that there is almost no damage to the surface under the remaining energy-flux densities. In order to ensure the crystallinity of the surface irradiated by femtosecond laser, the highest energy-flux density of laser irradiation was 0.65 kJ/m^2.

Fig. 6(a) shows an image of the activation rate of phosphorus under different energy-flux densities. The activation rate of phosphorus was almost the same under the energy-flux density of 0.3 kJ/m^2 and without laser irradiation. With the increase of the energy-flux density (> 0.3 KJ/m^2), the activation rate of phosphorus was increased. Under the energy-flux density of 0.65 KJ/m^2, the activation rate of phosphorus was the highest. The activation rate of phosphorus was increased from 67% to 74.81%. Fig. 6(b) reveals the reason for the change in the activation rate of phosphorus is that the change in the activated areal density of phosphorus impurities after laser irradiation. The SIMS measured results demonstrated that laser irradiation did not change the distribution of phosphorus diffusion. Thus, the areal density of phosphorus impurities before the junction depth of the SIMS tested was basically a fixed value, about 2.82×10^{15} cm^{-2}.

It can be seen from Fig. 7(a) that with the increase of the energy-flux density, the activated concentration of phosphorus was increased, and in the tail region of the curve, the activated concentration of phosphorus was increased significantly. Fig. 7(b) shows the change of activation rate with thickness under different energy-flux densities. With the increase of energy-flux density, the activation rate of phosphorus at each thickness was increased, but the increase of the activation rate was mainly reflected at depths of more than

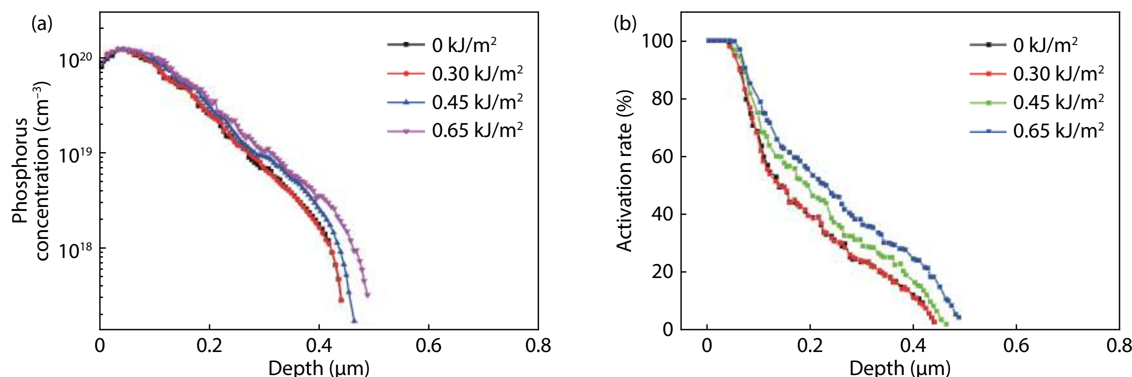

Fig. 7. (Color online) (a) ECV test results at different laser irradiation conditions. (b) Effective activation rate with thickness at different laser irradiation conditions.

100 nm. Additionally, in the absence of laser irradiation, the activation rate was about 50% at about 100 nm. Thus, when the thickness of crystalline silicon is above 100 nm, interstitial impurities of phosphorus dominate[9].

A speculation was proposed that laser irradiation can increase the activation rate of phosphorus impurities.

At present, the model of the silicon surface irradiated by the femtosecond laser is widely accepted as the plasma model, that is, the silicon will not melt during the laser irradiation, but a superfluid is generated[24]. Ho *et al.* found that the temperature of the material only rose to 600 K during laser irradiation[25], which is much lower than the melting point of silicon at 1685 K, which supported the non-thermal model. After femtosecond laser irradiation, a large number of electrons are excited, that is, a large number of valence band electrons are excited to the conduction band, which will weaken the covalent bonding of the silicon surface and lead to the silicon surface turning into the superfluid which has high coordination number and weak covalent bond. Therefore, the interstitial phosphorus can react with the adjacent silicon atoms to form activation phosphorus, thereby increasing the activation concentration and the activation rate of phosphorus.

4. Conclusion

Annealing experiments were conducted at different temperatures on silicon samples after implantation of phosphorus ions (energy = 55 keV, dose = 3×10^{15} cm^{-2}). The activation areal density of phosphorus impurities reached the highest at 850 °C. Simultaneously, the highest activation rate of 67% was obtained. This discovery is of great importance to the current industrial production. Yingli is now building a solar cell production line that uses ion implantation technology. This condition can be directly used in the production line. Experiments showed that the activated concentration of phosphorus at the surface was high. As the depth increases, the activated concentration was decreased, and the activation rate also was decreased.

When irradiating the samples with a femtosecond laser, the activation rate of phosphorus had a certain increase on the original basis. Without obvious damage to the sample surface, the activation rate of phosphorus was increased from 67% to 74.81%. This supported that the femtosecond laser can increase the activation rate of phosphorus. This provides a feasible method of improving the efficiency of crystalline silicon solar cells in the future.

Acknowledgements

This work was supported by National Key R&D Program of China (No. 2018YFB1500500). We thank Yingli Company and TEDA Institute of Applied Physics of Nankai University for their help in this research.

References

[1] Hofker W K. Implantation of boron in silicon. Philips Res Rep, 1975, 15(3), 189

[2] Skorupa W, Wieser E, Groetzschel R, et al. High energy implantation and annealing of phosphorus in silicon. Nucl Instrum Methods Phys Res, 1987, 19/20(Part1), 335

[3] Kisielewicz M A. The damage-dependent atom and carrier profiles in phosphorus-implanted silicon. Thin Solid Films, 1983, 109(1), 11

[4] Tsai M Y, Streetman B G. Recrystallization of implanted amorphous silicon layers. I. Electrical properties of silicon implanted with BF^{+2} or Si^{+}+B^{+}. J Appl Phys, 1979, 50(1), 183

[5] Landi E, Guimaraes S, Solmi S. Influence of nucleation on the kinetics of boron precipitation in silicon. Appl Phys A, 1987, 44(2), 135

[6] Solmi S, Landi E, Baruffaldi F. High-concentration boron diffusion in silicon: Simulation of the precipitation phenomena. J Appl Phys, 1990, 68(7), 3250

[7] Stolk P A, Gossmann H J, Eaglesham D J, et al. Physical mechanisms of transient enhanced dopant diffusion in ion-implanted silicon. J Appl Phys, 1997, 81(9), 6031

[8] Suzuki K, Tada Y, Kataoka Y, et al. Maximum active concentration of ion-implanted phosphorus during solid-phase epitaxial recrystallization. IEEE Trans Electron Devices, 2007, 54(8), 1985

[9] Hadjersi T. Annihilation kinetics of defects induced by phosphorus ion implantation in silicon. Appl Surf Sci, 2001, 185(1/2), 140

[10] Wu C, Crouch C H, Zhao L, et al. Near-unity below-band-gap absorption by microstructured silicon. Appl Phys Lett, 2001, 78(13), 1850

[11] Crouch C H, Carey J E, Shen M, et al. Infrared absorption by sulfur-doped silicon formed by femtosecond laser irradiation. Appl Phys A, 2004, 79(7), 1635

[12] Köhler J R, Eisele S J. Phosphorus out-diffusion in laser molten silicon. J Appl Phys, 2015, 117(14), 145701

[13] Winkler M T, Recht D, Sher M J, et al. Insulator-to-metal transition in sulfur-doped silicon. Phys Rev Lett, 2011, 106(17), 51

[14] Normann H B, Svensson B G, Monakhov E. Formation of shallow front emitters for solar cells by rapid thermal processing. Phys Status Solidi, 2012, 9(11), 2138

[15] Uematsu M. Simulation of boron, phosphorus, and arsenic diffusion in silicon based on an integrated diffusion model, and the an-

omalous phosphorus diffusion mechanism. J Appl Phys, 1997, 82(5), 2228

[16] Othonos A. Probing ultrafast carrier and phonon dynamics in semiconductors. J Appl Phys, 1998, 83(4), 1789

[17] Cerva H. Comparison of transmission electron microscope cross sections of amorphous regions in ion implanted silicon with point-defect density calculations. J Electrochem Soc, 1992, 139(12), 3631

[18] Uematsu M. Implantation species dependence of transient enhanced diffusion in silicon. J Appl Phys, 1998, 83(1), 120

[19] Schroer E, Uematsu M. Simulation of clustering and pile-up during post-implantation annealing of phosphorus in silicon. Jpn J Appl Phys, 1999, 38(1A), 7

[20] Uematsu M. Simulation of clustering and transient enhanced diffusion of boron in silicon. J Appl Phys, 1998, 84(9), 4781

[21] Uematsu M. Simulation of high-concentration phosphorus diffusion in silicon taking into account phosphorus clustering and pile-up. Jpn J Appl Phys, 1999, 38(11), 6188

[22] Mayer J W, Nicolet M, Chu W K. Backscattering spectrometry. Academic Press, 1978

[23] Sundaram S K, Mazur E. Inducing and probing non-thermal transitions in semiconductors using femtosecond laser pulses. Nat Mater, 2002, 1(4), 271

[24] Silvestrelli P L, Alavi A, Parrinello M, et al. Ab initio molecular dynamics simulation of laser melting of silicon. Phys Rev Lett, 1996, 77(15), 3149

[25] Lo H W, Compaan A. Raman measurement of lattice temperature during pulsed laser heating of silicon. Phys Rev Lett, 1980, 44(24), 1604